

Article

Research on the Motion Error Analysis and Compensation Strategy of the Delta Robot

Deyong Shang ¹, Yu Li ^{1,*}, Yue Liu ² and Shuanwei Cui ¹

¹ College of Mechanical and Information Engineering, China University of Mining and Technology (Beijing), Beijing 100083, China; shangdeyong@cumtb.edu.cn (D.S.); cuishuanwei@outlook.com (S.C.)

² State Key Laboratory of Tribology, Department of Mechanical Engineering, Tsinghua University, Beijing 100084, China; liuyue2018@mail.tsinghua.edu.cn

* Correspondence: liyu1512443766@163.com; Tel.: +86-13126758001

Received: 25 March 2019; Accepted: 6 May 2019; Published: 8 May 2019



Abstract: The Delta robots are widely used in packaging, sorting, precision positioning, and other fields. Motion accuracy is an important indicator for evaluating robot performance. However, due to the existence of mechanism errors, the motion accuracy of the robot will be reduced. Therefore, how to reduce motion errors and improve accuracy are important issues for robots. The purpose of the present study is to analyze the motion error and propose an error compensation scheme to improve the motion accuracy of the robot. Firstly, the kinematic model of the robot is established by the D-H matrix transformation method. An error model considering dimension error, the error of revolute joint clearance, driving error, and the error of spherical joint clearance is established. Additionally, the influence of different errors on the motion accuracy is analyzed. Secondly, an error compensation strategy of controlling the driving angle is proposed. The analysis of error compensation is carried out by a numerical example. Comparing the results before and after compensation, it is known that the robot can move along the desired position, so the motion error of the robot is compensated, which proves that this method is effective for improving the motion accuracy of the robot.

Keywords: Delta robot; motion accuracy; kinematic model; error analysis; error compensation

1. Introduction

Compared with serial robots, parallel robots have the advantages of large carrying capacity, good motion performance, fast moving speed, etc. [1–4]. Delta parallel robots [5] are widely used in assembly detection, packaging, precision positioning, and other fields. People's demand for accuracy in parallel robots is also increasing. Motion accuracy is an important index to evaluate the quality of mechanisms [6,7]. However, due to the existence of the mechanism errors, the end effector of the robot will produce certain motion error, which will reduce the motion accuracy of the mechanism. Therefore, how to compensate the error and improve motion accuracy of the robot has become an important research issue.

Aimed at the motion accuracy of robots, Xu established the error model and performed a kinematic reliability and sensitivity analysis of the modified Delta robot. However, the influence of the clearance error is not considered in the paper, and the error compensation method is not further proposed [8]. Bai et al. deals with kinematic calibration of the Delta robot using distance measurements. A linearized compensator for real-time error compensation is designed in the paper. The experimental results show that the method can improve the positioning accuracy of the robot [9]. Zhou et al. established the coordinate system of the robot and took into account the errors introduced by the joint parameters of the robot, established the pose error model of the robot, and proposed a precision compensation method for industrial robots based on spatial interpolation [10,11]. Peng proposed a method of controlling the

driving angle to compensate the error of the robot. A new type of trajectory planning and positioning error compensation interface for the serial robot was developed [12]. The results showed that the compensation effect of positioning error was good, which provides an effective method for improving the positioning accuracy of robots. Vischer and Clavel proposed a method of error calibration and established the parametric model of the Delta robot by the vector method. The kinematics calibration of the robot is carried out by implicit calibration and semi-parametric calibration. The kinematic error of the robot is reduced and the kinematic precision is improved by calibration [13]. Wang [14] proposed a robot manipulator calibration method using a camera-based measurement system and a neural network algorithm. A neural network model is utilized to approximate the error surface. A significant improvement in accuracy is obtained by the proposed techniques in comparison with traditional bilinear analytical methods.

Among the existing literature, a great deal of research has focused on the dimension errors of the components, while few studies considered the clearance errors. Since parallel mechanisms are used in high-speed situations, the error of joint clearance will reduce the kinematic accuracy and motion stability of mechanisms, so the influence of the clearance error should be considered. In addition, robot accuracy compensation can be divided into two methods according to different control methods: one is to increase the end feedback detection and achieve full closed-loop control [15,16]. This method usually uses the embedded control method to integrate the laser tracker, robot, and control computer to quickly and instantaneously feedback the pose of the robot, thereby improving the positioning accuracy. The other method is to improve the absolute positioning accuracy by calibration. These methods have a certain compensation effect, but require higher experimental conditions.

The purpose of the present study is to analyze the motion error and propose an error compensation strategy to improve the motion accuracy of the robot. Firstly, the kinematic model of the robot is established by the D-H matrix transformation method. An error model considering dimension error, the error of revolute joint clearance, driving error, and the error of spherical joint clearance is established. And the influence of different errors on the motion accuracy is analyzed. Secondly, this paper intends to apply the method of controlling the driving angle to the Delta parallel robot. An error compensation strategy is proposed. Then the error compensation analysis of the robot is carried out and the effectiveness of the strategy is verified by numerical examples.

2. The Coordinate System of the Delta Parallel Mechanism

The structural model of the Delta parallel robot is shown in Figure 1, and the kinematic chain of the Delta parallel robot is shown in Figure 2.

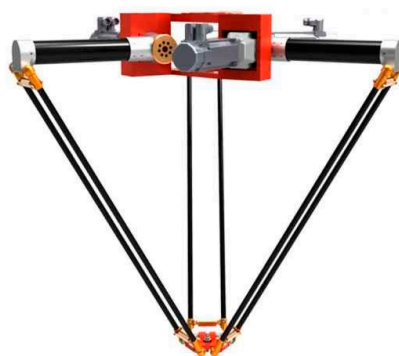


Figure 1. The structural model of the robot.

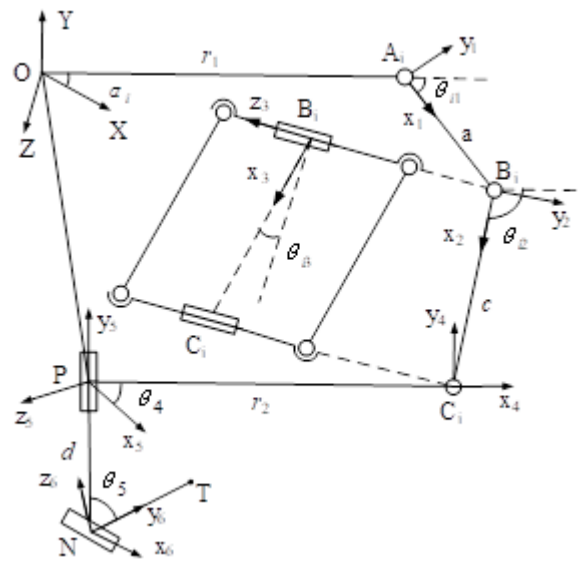


Figure 2. Motion diagram of the kinematic chain.

The global coordinate system O-XYZ is located at the center point of the fixed platform at point O. The X axis points to the OA₁, the Y axis is perpendicular to the platform surface, and the negative direction of the Y axis is the gravity direction of the moving platform.

The position of the rotating pair on the fixed platform and the moving platform is arranged in a triangle, of which the circumradius is respectively r_1 and r_2 . The length of the driving arm A_iB_i is a , and the length of the parallelogram mechanism (the driven arm B_iC_i) is c . The length of PN of the mechanism is d (PN is the distance between the center point P of the moving platform and the origin N of the local coordinate system). α_i is the angle between the OA_i and the global coordinate X axis, which is shown in the diagram. When the corresponding kinematic chain i is 1, 2, 3, α_i is 0° , 120° , and 240° , respectively. The input angle (driving angle) is θ_{i1} , θ_{i4} , θ_{i5} , and the rotation angle of driven arm is θ_{i2} . The swing angle of driven arm is θ_{i3} . Point N is the origin of $(xyz)_6$ in the local coordinate system. Point T is the working position.

3. Modeling of Mechanism Position Error

According to the structural characteristics of the delta parallel robot, it can be seen that the sources of the position error of the mechanism are mainly in the following categories:

- (1) Dimension error;
- (2) The error of revolute joint clearance;
- (3) Driving error; and
- (4) The error of spherical joint clearance.

3.1. Considering Dimension Error

According to the homogeneous transformation rule, we can get the homogeneous transformation matrix between local coordinate systems, as shown in Table 1.

$$\mathbf{M}(x, r_1) = \begin{bmatrix} 1 & 0 & 0 & r_1 \\ 0 & 1 & 0 & 0 \\ 0 & 0 & 1 & 0 \\ 0 & 0 & 0 & 1 \end{bmatrix} \quad (1)$$

$$\mathbf{R}(y, \alpha_i) = \begin{bmatrix} \cos \alpha_i & 0 & \sin \alpha_i & 0 \\ 0 & 1 & 0 & 0 \\ -\sin \alpha_i & 0 & \cos \alpha_i & 0 \\ 0 & 0 & 0 & 1 \end{bmatrix} \tag{2}$$

Table 1. Homogeneous transformation matrix between local coordinate systems.

Local Coordinate System	Variable θ_i	Homogeneous Transformation Matrix
$(xyz)_1$	θ_{i1}	${}^0\mathbf{T}_1 = \mathbf{R}(y, \alpha_i)\mathbf{M}(x, r_1)\mathbf{R}(z, -\theta_{i1})$
$(xyz)_2$	θ_{i2}	${}^1\mathbf{T}_2 = \mathbf{R}(x, a)\mathbf{M}(z, \theta_{i1})\mathbf{R}(z, -\theta_{i2})$
$(xyz)_3$	θ_{i3}	${}^2\mathbf{T}_3 = \mathbf{R}(y, \theta_{i3})$
$(xyz)_4$	None	${}^3\mathbf{T}_4 = \mathbf{M}(x, c)\mathbf{R}(y, -\theta_{i3})\mathbf{R}(z, \theta_{i2})$
$(xyz)_5$	θ_4	${}^4\mathbf{T}_5 = \mathbf{M}(x, -r_2)\mathbf{R}(y, -\alpha_i)\mathbf{R}(y, \theta_4)$
$(xyz)_6$	θ_5	${}^5\mathbf{T}_6 = \mathbf{M}(y, -d)\mathbf{R}(x, \theta_5)$

Note: $\mathbf{M}(x, r_1)$ represents a homogeneous transformation matrix that translates r_1 unit vectors along the x -axis of the local coordinate system. $\mathbf{R}(y, \alpha_i)$ represents the homogeneous transformation matrix that rotates the α_i angle around the y -axis of the local coordinate system. For instance, the expressions of $\mathbf{M}(x, r_1)$ and $\mathbf{R}(y, \alpha_i)$ are as follows. The rest are similar and the same is available.

Therefore, the homogeneous transformation matrix ${}^0\mathbf{T}_6$ of the coordinate system $(xyz)_6$ relative to the global coordinate system $(XYZ)_O$ can be expressed in two ways as follows:

$$\begin{aligned} {}^0\mathbf{T}_6 &= \prod_{k=1}^6 {}^{k-1}\mathbf{T}_k \\ &= \begin{bmatrix} \cos \theta_4 & \sin \theta_5 \sin \theta_4 & \cos \theta_5 \sin \theta_4 \\ 0 & \cos \theta_5 & -\sin \theta_5 \\ -\sin \theta_4 & \sin \theta_5 \cos \theta_4 & \cos \theta_5 \cos \theta_4 \\ 0 & 0 & 0 \end{bmatrix} \tag{3} \\ &\quad \left. \begin{array}{l} a \cos \alpha_i \cos \theta_{i1} + c(\cos \alpha_i \cos \theta_{i2} \cos \theta_{i3} - \sin \alpha_i \sin \theta_{i3}) + (r_1 - r_2) \cos \alpha_i \\ -d - c \sin \theta_{i2} \cos \theta_{i3} - a \sin \theta_{i1} \\ -a \sin \alpha_i \cos \theta_{i1} - c(\cos \alpha_i \sin \theta_{i3} + \sin \alpha_i \cos \theta_{i2} \cos \theta_{i3}) + (r_2 - r_1) \sin \alpha_i \\ 1 \end{array} \right\} \end{aligned}$$

Let Equation (3) be transformed as follows:

$\mathbf{R}(y, \alpha_i)^{-1} {}^0\mathbf{T}_6 \mathbf{R}(x, \theta_5)^{-1} \mathbf{M}(y, -d)^{-1} \mathbf{R}(y, \theta_4)^{-1} \mathbf{R}(y, -\alpha_i)^{-1}$. The converted matrix is denoted as \mathbf{T} . We can obtain:

$$\mathbf{T} = \begin{bmatrix} 1 & 0 & 0 & x \cos \alpha_i - z \sin \alpha_i \\ 0 & 1 & 0 & d + y \\ 0 & 0 & 1 & x \sin \alpha_i + z \cos \alpha_i \\ 0 & 0 & 0 & 1 \end{bmatrix} \tag{4}$$

$$\mathbf{T} = \begin{bmatrix} 1 & 0 & 0 & r_1 - r_2 + c \cos \theta_{i2} \cos \theta_{i3} + a \cos \theta_{i1} \\ 0 & 1 & 0 & -c \sin \theta_{i2} \cos \theta_{i3} - a \sin \theta_{i1} \\ 0 & 0 & 1 & -c \sin \theta_{i3} \\ 0 & 0 & 0 & 1 \end{bmatrix} \tag{5}$$

From Equations (4) and (5), we can obtain:

$$\begin{cases} x = -c \sin \theta_{i3} \sin \alpha_i + r_1 \cos \alpha_i - r_2 \cos \alpha_i \\ \quad + a \cos \theta_{i1} \cos \alpha_i + c \cos \theta_{i2} \cos \theta_{i3} \cos \alpha_i \\ y = -a \sin \theta_{i1} - c \sin \theta_{i2} \cos \theta_{i3} - d \\ z = -c \sin \theta_{i3} \cos \alpha_i - r_1 \sin \alpha_i + r_2 \sin \alpha_i \\ \quad - a \cos \theta_{i1} \sin \alpha_i - c \cos \theta_{i2} \cos \theta_{i3} \sin \alpha_i \end{cases} \tag{6}$$

Equation (6) is the relationship between the end output position and the structural parameters in the ideal case. In fact, the parameters of each structure have certain deviations due to the influence of various factors.

The Taylor series expansion is carried out at each parameter of Equation (6). The expression is obtained as follows:

$$\left\{ \begin{array}{l} \Delta x^o = \sum_{i=1}^3 (\cos \alpha_i \Delta r_{i1} - \cos \alpha_i \Delta r_{i2} + \cos \theta_{i1} \cos \alpha_i \Delta a_i \\ \quad + (\cos \theta_{i2} \cos \theta_{i3} \cos \alpha_i - \sin \theta_{i3} \sin \alpha_i) \Delta c_i \\ \quad + (-r_{i1} \sin \alpha_i + r_{i2} \sin \alpha_i - a_i \cos \theta_{i1} \sin \alpha_i \\ \quad - c_i \cos \theta_{i2} \cos \theta_{i3} \sin \alpha_i - c_i \sin \theta_{i3} \cos \alpha_i) \Delta \alpha_i) \\ \Delta y^o = - \sum_{i=1}^3 (\sin \theta_{i1} \Delta a_i + \sin \theta_{i2} \cos \theta_{i3} \Delta c_i) - \Delta d \\ \Delta z^o = \sum_{i=1}^3 (-\sin \alpha_i \Delta r_{i1} + \sin \alpha_i \Delta r_{i2} - \cos \theta_{i1} \sin \alpha_i \Delta a_i \\ \quad - (\cos \theta_{i2} \cos \theta_{i3} \sin \alpha_i + \sin \theta_{i3} \cos \alpha_i) \Delta c_i \\ \quad + (-r_{i1} \cos \alpha_i + r_{i2} \cos \alpha_i - a_i \cos \theta_{i1} \cos \alpha_i \\ \quad - c_i \cos \theta_{i2} \cos \theta_{i3} \cos \alpha_i + c_i \sin \theta_{i3} \sin \alpha_i) \Delta \alpha_i) \end{array} \right. \quad (7)$$

The relation between the input error and the output error of the mechanism is obtained from Equation (7).

According to the above equation, the error sources are Δr_{i1} , Δr_{i2} , Δa_i , Δc_i , $\Delta \alpha_i$, etc. Moreover, there are also errors in revolute joints, driving errors, and errors in spherical joints.

3.2. Considering the Error of Revolute Joint Clearance

The existence of clearances in these joints is inevitable due to machining tolerances, wear, and material deformation. The revolute joint of the Delta robot is composed of a sleeve hole and a shaft. The error of the revolute joint is the difference between the radii of the two components, that is, the clearance error is the radial error of the revolute joint. Therefore, the planar model is used to describe the clearance of the revolute joint, as shown in Figure 3.

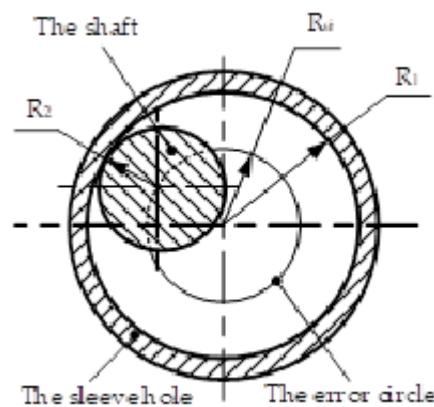


Figure 3. Model of revolute joint.

The error circle is the circle with a radius of R_{ei} . From the model of revolute joint, we can obtain:

$$R_{ei} = R_1 - R_2, \quad (8)$$

where R_1 and R_2 are radii of the sleeve hole and the shaft.

This paper only considers the clearance error between the revolute joint of the platform and the driving arm. According to the effective length theory [17], the clearance error R_{ei} of the revolute joint

is equivalent to the change in length of the driving arm Δa . Namely, $R_{ei} = \Delta a$. Therefore, the error caused by the revolute joint is as follows:

$$\begin{cases} \Delta x^R = \sum_{i=1}^3 \cos \theta_{i1} \cos \alpha_i R_{ei} \\ \Delta y^R = -\sum_{i=1}^3 \sin \theta_{i1} R_{ei} \\ \Delta z^R = -\sum_{i=1}^3 \cos \theta_{i1} \sin \alpha_i R_{ei} \end{cases} \quad (9)$$

3.3. Considering Driving Error

The input angle θ_{i1} is the driving angle of the mechanism at any moment. The first-order Taylor series expansion of the Equation (6) at θ_{i1} . Therefore, the error caused by driving error is as follows:

$$\begin{cases} \Delta x^D = \sum_{i=1}^3 -a \sin \theta_{i1} \cos \alpha_i \Delta \theta_{i1} \\ \Delta y^D = \sum_{i=1}^3 -a \cos \theta_{i1} \Delta \theta_{i1} \\ \Delta z^D = \sum_{i=1}^3 a \sin \theta_{i1} \sin \alpha_i \Delta \theta_{i1} \end{cases} \quad (10)$$

3.4. Considering the Error of Spherical Joint Clearance

The structure of spherical joint is composed of spherical shell and sphere. The structure of the spherical joint is shown in Figure 4. When the robot works, the sphere moves in the spherical shell, and the motion model at this time is a spatial model. Ideally, the spherical center of the sphere is located at point O. Since the clearance is inevitable, the spherical center is actually located at point O'. In this case, the distance between the center of the sphere and the origin is the clearance of the spherical joint.

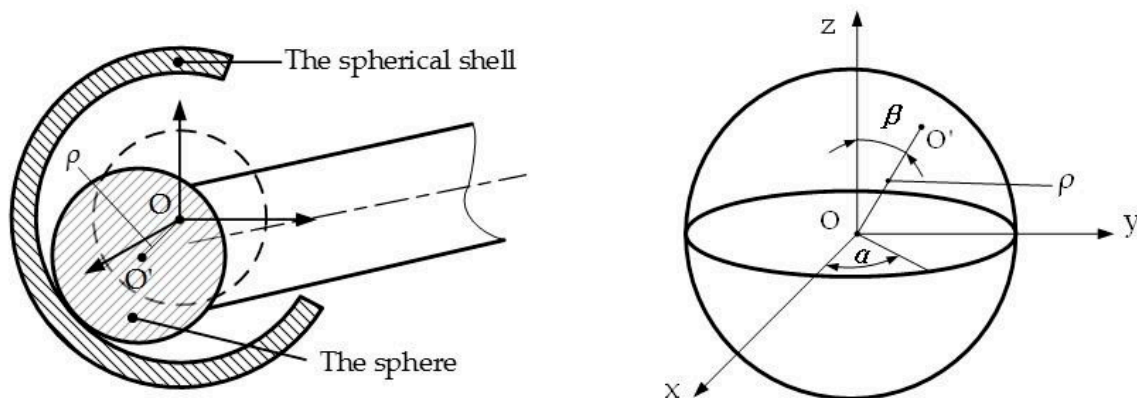


Figure 4. Model of the spherical joint.

The error of the spherical joint affects the output error of the Delta parallel robot. The spherical joint constrains the translational freedom in three directions, while it does not limit the rotational degree of freedom. Therefore, the error caused by the clearance between the spherical joint is only three translational errors [18]. Namely, the errors in the x , y , and z directions are Δx , Δy , Δz , respectively.

When the clearance error of the spherical joint is ρ , the angle between the projection in the xy plane of ρ and the x axis is α , and the angle between the clearance direction and the z axis is β . The errors of the spherical joint in the x , y , and z directions are as follows:

$$\begin{cases} \Delta x^Q = \rho \sin \beta \cos \alpha \\ \Delta y^Q = \rho \sin \beta \sin \alpha \\ \Delta z^Q = \rho \cos \beta \end{cases} \quad (11)$$

According to the structural diagram of the Delta parallel mechanism, it is known that the clearance ρ of spherical joint is equivalent to the change in length of the parallelogram mechanism (driven arm) rod Δc . Namely, $\rho = \Delta c$. Therefore, the position error of the end effector caused by the spherical joint is equivalent to the output error considering Δc . Thus, it can be obtained:

$$\begin{cases} \Delta x^Q = \sum_{i=1}^3 (\cos \theta_{i2} \cos \theta_{i3} \cos \alpha_i - \sin \theta_{i3} \sin \alpha_i) \rho \\ \Delta y^Q = -\sum_{i=1}^3 \sin \theta_{i2} \cos \theta_{i3} \rho \\ \Delta z^Q = -\sum_{i=1}^3 (\cos \theta_{i2} \cos \theta_{i3} \sin \alpha_i + \sin \theta_{i3} \cos \alpha_i) \rho \end{cases} \quad (12)$$

From the above analysis, the total position error of the end effector in the x, y and z directions is the superposition of the four kinds of errors above at any time. Thus, it can be obtained:

$$\Delta q = \Delta q^O + \Delta q^R + \Delta q^D + \Delta q^Q = \sum_{i=1}^n Kq_{si} \Delta s_i, q = x, y, z. \quad (13)$$

In Equation (13), Kq_{si} is the error transfer coefficient of Δs_i .

The value of Kq_{si} is usually determined by the posture and structural parameters of the mechanism together. The value of Kq_{si} can quantitatively reflect the degree of the influence of error Δs_i on the motion accuracy of the robot.

4. Error Compensation Strategy

4.1. Error Synthesis of the Robot

Since the influence of each error source is independent with each other, the total error of the end effector is the sum of the error values caused by the error sources. According to Equation (13), the total error caused in x, y , and z direction is $\Delta x, \Delta y$, and Δz , respectively. Based on the error model of the mechanism, the positioning error of the end effector can be obtained, which provides a data basis for error compensation.

In addition, because errors such as $\Delta r_{i1}, \Delta r_{i2}, \Delta a_i, \Delta c_i, \Delta \alpha_i, R_{ei}, \rho$ belong to structural errors, they are mainly produced by the process of manufacturing and assembly, etc. These errors are unavoidable, and the cost of improving motion accuracy by controlling these errors is too high and the effect is not obvious. Therefore, the total error caused by each error source is equivalent to the angle of the driving arm, and the error compensation is realized by controlling the driving angle, then the motion accuracy of the robot is improved.

4.2. Error Compensation Principle

The schematic diagram of error compensation is shown in Figure 5, where P is the desired position.

When the end effector of the robot reaches the desired position P , the theoretical value of driving angle θ_{i1} can be calculated by the inverse kinematic equation. The calculation process of the driving angle θ_{i1} is as follows:

From Equations (4) and (5), it is known that:

$$\mathbf{T} = \begin{bmatrix} 1 & 0 & 0 & x \cos \alpha_i - z \sin \alpha_i \\ 0 & 1 & 0 & d + y \\ 0 & 0 & 1 & x \sin \alpha_i + z \cos \alpha_i \\ 0 & 0 & 0 & 1 \end{bmatrix}, \mathbf{T} = \begin{bmatrix} 1 & 0 & 0 & r_1 - r_2 + c \cos \theta_{i2} \cos \theta_{i3} + a \cos \theta_{i1} \\ 0 & 1 & 0 & -c \sin \theta_{i2} \cos \theta_{i3} - a \sin \theta_{i1} \\ 0 & 0 & 1 & -c \sin \theta_{i3} \\ 0 & 0 & 0 & 1 \end{bmatrix}.$$

Setting $t_x = x \cos \alpha_i - z \sin \alpha_i, t_y = d + y, t_z = x \sin \alpha_i + z \cos \alpha_i$, we can obtain:

$$\theta_{i1} = 2\arctan\left(\frac{-t_{i1} \pm \sqrt{t_{i1}^2 - 4t_{i2}t_{i0}}}{2t_{i2}}\right),$$

where:

$$t_{i2} = b_0^2 - k_0^2 - a^2 - t_y^2 - 2ak_0, \\ t_{i1} = -4at_y, t_{i0} = b_0^2 - k_0^2 - a^2 - t_y^2 + 2ak_0, b_0 = c \cos \theta_{i3}, k_0 = t_x - r_1 + r_2$$

Thus, the driving angle θ_{i1} is obtained by the inverse equation of the robot.

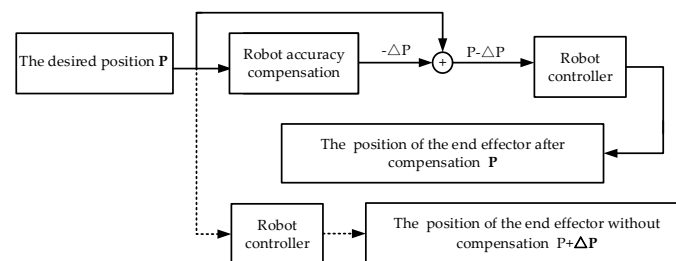


Figure 5. The schematic diagram of error compensation.

However, due to various error factors of the mechanism, there are differences between the actual kinematic parameters and theoretical values. Therefore, there are deviations between the actual trajectory and the theoretical trajectory of the robot. Therefore, when the driving angle θ_{i1} obtained by the inverse solution is used to drive the robot, the deviation between the actual position and the desired position is the position error of the robot. The position error is denoted as ΔP . In three directions, ΔP can be calculated from Equation (13). Thus, when no error compensation is performed, the actual position of the robot is $P + \Delta P$.

In order to compensate for the positioning error of the robot due to the parameter errors, the desired position P is replaced by the position $P - \Delta P$ by biasing a numerical value $-\Delta P$, that is, the inverse solution is calculated with $P - \Delta P$ instead of P , and then the driving angle θ_{i1}' of the inverse solution is used to drive the robot. Then the motion error $\Delta P'$ caused by the mechanism errors and the bias $-\Delta P$ will cancel out, If the first compensation does not reach the predetermined accuracy, the second compensation can be made on the basis of the first compensation. The actual position of the robot will be closer to the desired position P . The compensation is completed until the desired accuracy is achieved. The results of the first compensation provide the data basis for the second compensation. This is the principle of error compensation for the mechanism.

5. Numerical Example

The structure parameters of the Delta parallel mechanism are as follows: $r_1 = 200$ mm, $r_2 = 200$ mm, $a = 200$ mm, $c = 400$ mm, $\alpha_1 = 0^\circ, \alpha_2 = 120^\circ, \alpha_3 = 240^\circ, \beta = 0^\circ$. The trajectory of the center point of the mechanism end actuator is as follows: $x = 30 \sin(120^\circ t)$ (mm), $y = -500 - 20t$ (mm), $z = -30 \cos(120^\circ t) + 30$ (mm), and the exercise time is 3 s. The position error of the mechanism is related to the following error sources: $\Delta r_{i1}, \Delta r_{i2}, \Delta a_i, \Delta c_i, \Delta \alpha_i, \Delta \theta_{i1}, R_{ei}, \rho$. The original input errors of the mechanism is shown in Table 2.

According to the error expressions, the error transfer coefficient of the error sources can be obtained. For instance, The error transfer coefficient of length error of the driving arm Δa_i and the driving angle $\Delta\theta_{i1}$ in x , y , and z direction is shown in Figures 6 and 7.

Table 2. Numerical values of input errors.

Original Input Errors($i = 1,2,3$)	Numerical Value
Dimension error of the fixed platform $\Delta r_{i1}/\text{mm}$	0.02
Dimension error of the moving platform $\Delta r_{i2}/\text{mm}$	0.02
Length error of the driving arm $\Delta a_i/\text{mm}$	0.02
Length error of the driven arm $\Delta c_i/\text{mm}$	0.02
Installation error $\Delta\alpha_i/\text{rad}$	0.02
Driving error $\Delta\theta_{i1}/\text{rad}$	0.02
The error of revolute joint clearance R_{ei}/mm	0.02
The error of spherical joint clearance ρ/mm	0.02

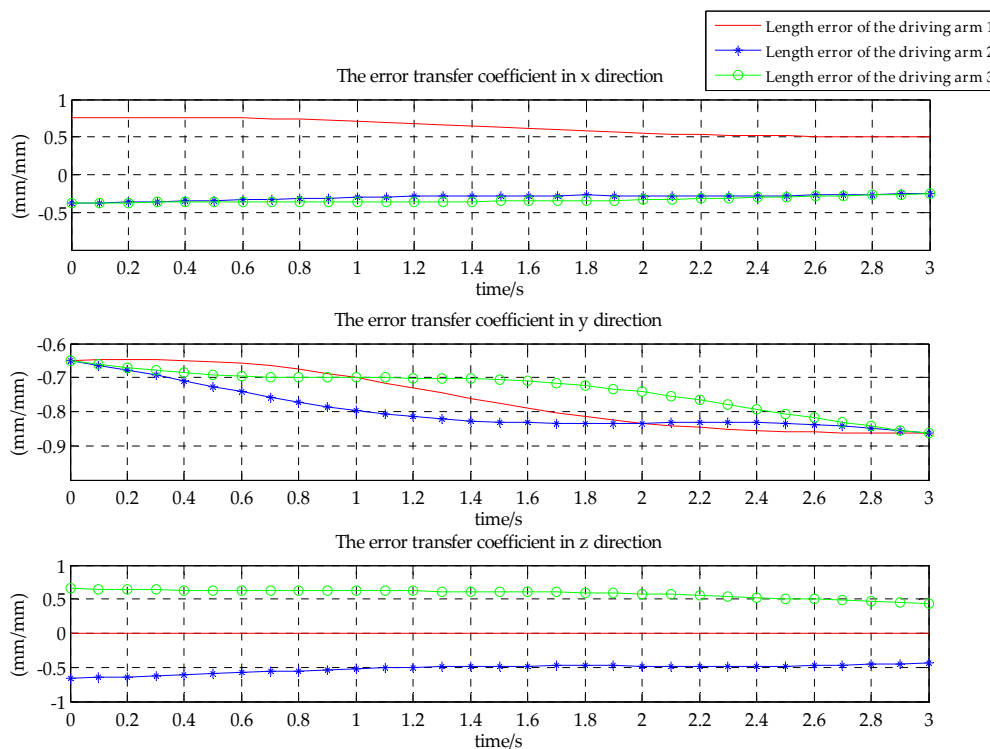


Figure 6. The error transfer coefficient of the length error of the driving arm Δa_i in x , y , and z directions.

Similarly, the error transfer coefficient graphs of other error sources can be obtained, but are omitted here.

According to the simulation results, it can be seen that the error transfer coefficient of the driving angle $\Delta\theta_{i1}$ is obviously larger than that of other error sources. Driving error is the main factor affecting the position error of the mechanism. The influence of driving error on motion accuracy of the mechanism is decisive, so it should be strictly controlled. The effect of the other mechanism errors on motion accuracy is small, moreover, the effect on the motion error is compensatory.

The total error in x , y , and z directions varies with time as follows:

From the given values of the original input errors in Table 2 and the results of the previous analysis, the total errors in three directions can be obtained from Equation (13), which is shown in Figure 8.

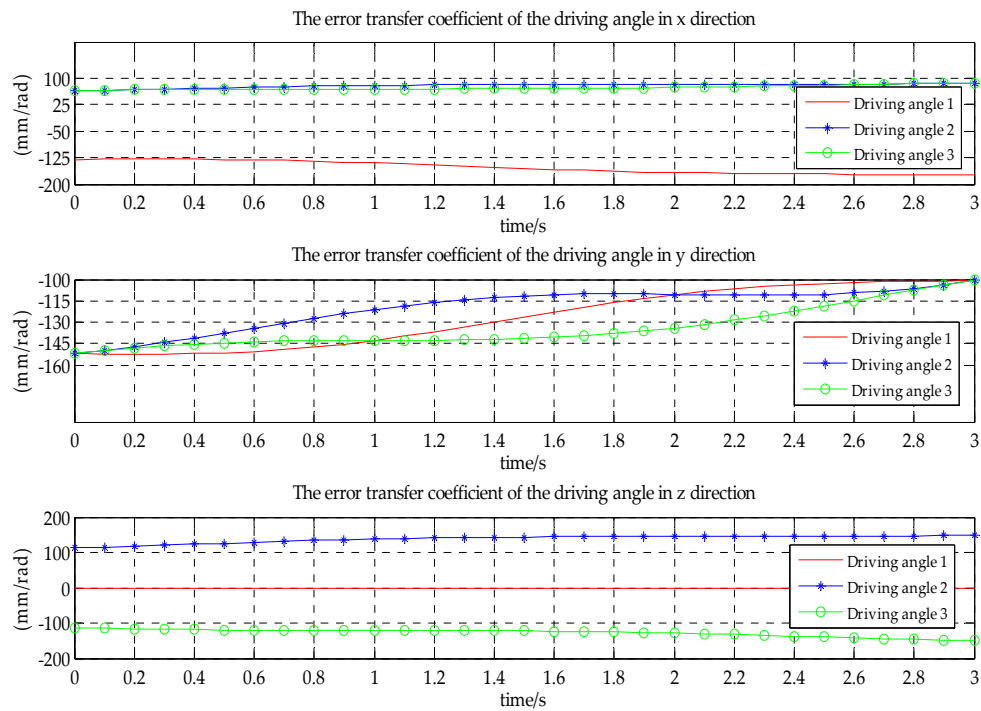


Figure 7. The error transfer coefficient of the driving angle $\Delta\theta_{i1}$ in x , y , and z directions.

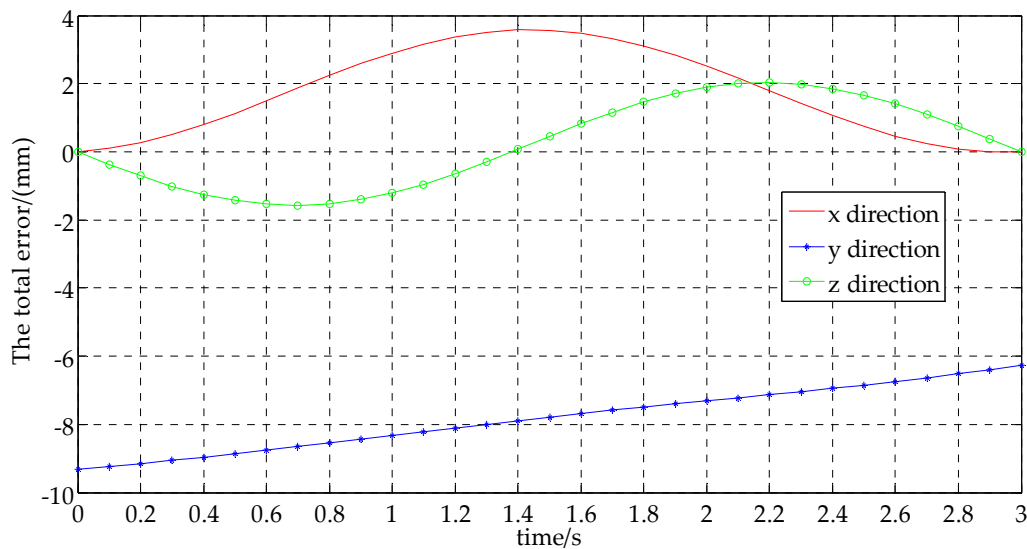


Figure 8. The total error in x , y , and z directions.

The data and curves of the errors in three directions are interpolated and fitted respectively, and the fitting equations of the errors in each direction can be obtained.

It can be seen from the curves of actual errors over time that the curves in the three directions conform to the compound expression of trigonometric function and polynomial function. Setting the corresponding parameter value, through interpolation calculation and analysis, the fitting error curve equation in the x direction is $\Delta x = -2.22(x - 0.25)(x - 2.75)$.

The fitting error curve equation in the y direction is $\Delta y = t - 9.35$.

The fitting error curve equation in the z direction is $\Delta z = -1.5 \sin(\frac{2\pi}{3}t + \frac{\pi}{18}) + 0.1t^2 + 0.03$.

Compared with the actual error curve, the fitting curve of the error equation is basically consistent with the actual error curve, so the error fitting equation can basically reflect the variation of the actual error.

The actual trajectory equation of robot end effector is:

$$\begin{cases} x' = x - \Delta x \\ y' = y - \Delta y \\ z' = z - \Delta z \end{cases} \quad (14)$$

The driving angle θ_{i1} is obtained by the inverse equation of the motion of the robot. Thus, the change of the driving angle with time before and after compensation is shown in Figure 9.

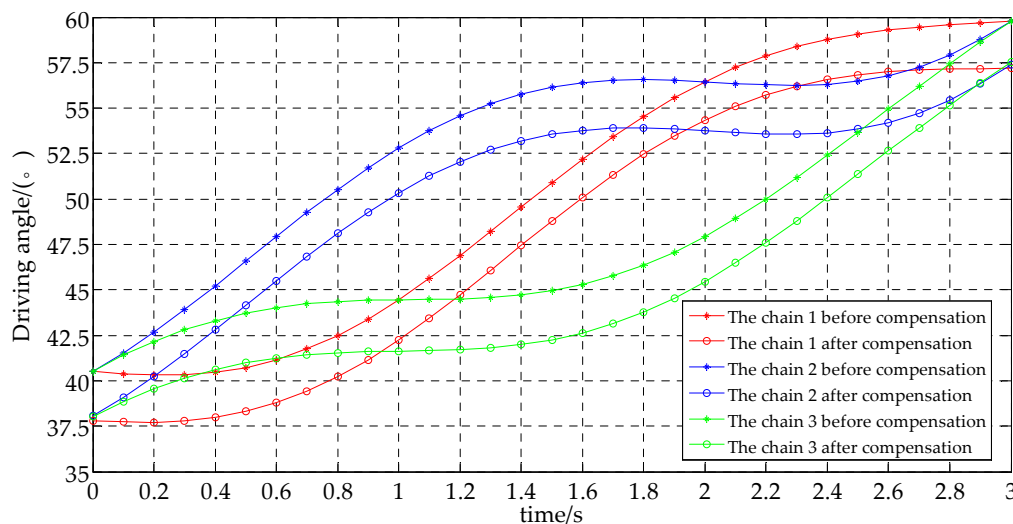


Figure 9. The change of the driving angle before and after compensation.

From Figure 9, the change of the driving angle θ_{i1} of the driving arm before and after compensation is consistent with time. Compared with the values of Figure 9, the initial and final values of the driving angle before compensation are 40.5° , 59.8° , and the initial and final values of the driving angle after compensation are 38° and 57.4° , respectively. Therefore, the compensation value of the driving angle is $40.5^\circ - 38^\circ + 1.1^\circ = 3.6^\circ$. Thus, the initial value of the steering angle of the control arm is $40.5^\circ - 3.6^\circ = 36.9^\circ$. From the obtained result, the rotation angle of the driving arm is brought to the set requirement by controlling the movement of the motor.

When the mechanism is driven by the driving angle after compensation, the displacement curves in x , y , and z direction before and after compensation are shown in Figure 10. The displacement data are shown in Appendix A.

The motion trajectory in space of the end effector before and after the compensation is shown in Figure 11.

From the Figures 10 and 11, comparing with the results before and after compensation, it can be seen that the motion trajectory after compensation is close to the desired position of the robot. The robot can move along the desired position, so that the error compensation of the robot is realized. It is proved that this method is effective and provides theoretical reference for the error compensation.

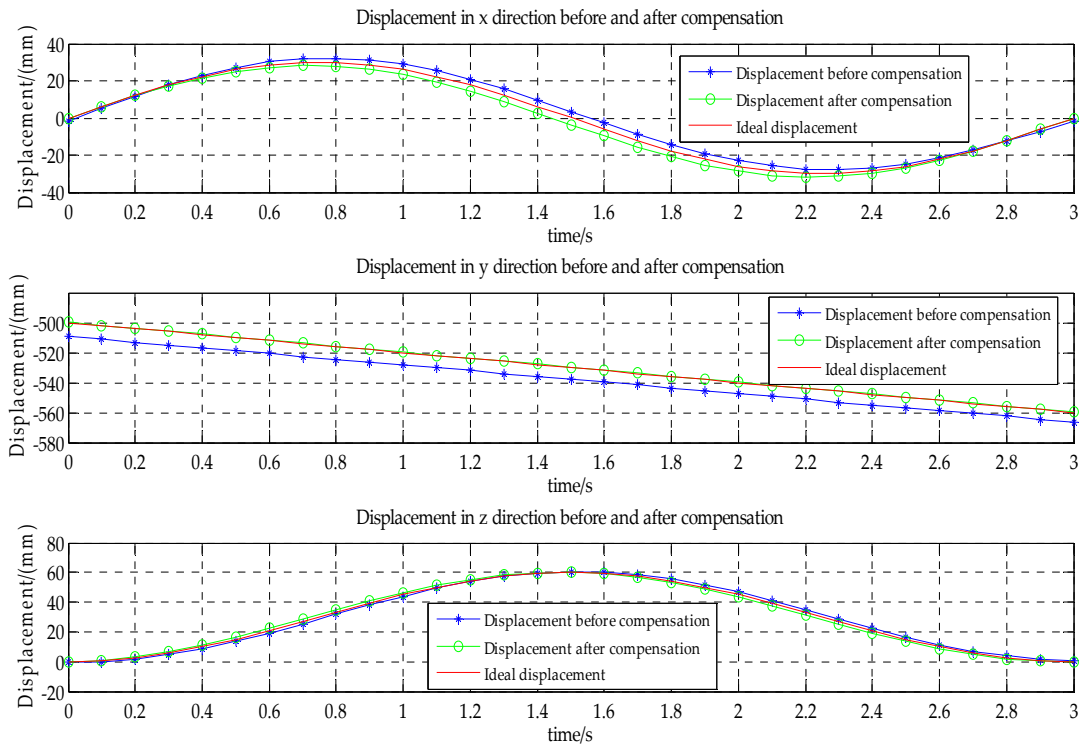


Figure 10. Displacement curves in x , y , and z directions before and after error compensation.

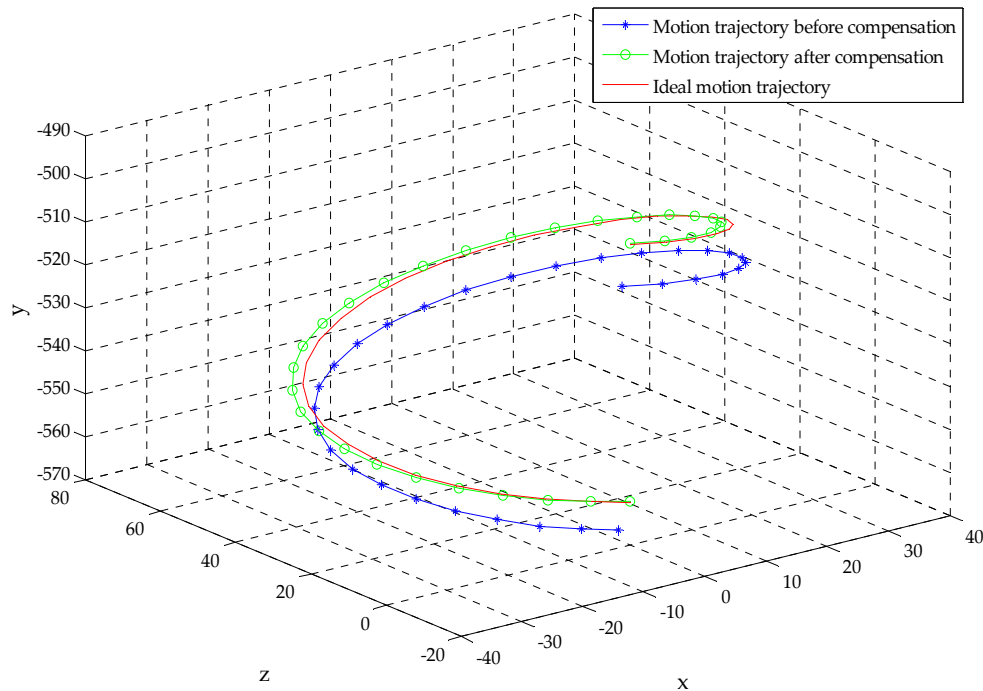


Figure 11. The motion trajectory in space of the end effector before and after compensation.

6. Conclusions

This paper establishes the kinematic model and the error mathematical model of the Delta robot and analyzes the influence of four main error sources on the position error of the mechanism. From the data analysis, it can be seen that the error transfer coefficient of the driving angle is obviously larger than that of other error sources. Driving error is the main factor affecting the position error of the mechanism. Moreover, an error compensation strategy of controlling the driving angle is proposed.

The analysis of error compensation is carried out by a numerical example. Comparing the results before and after compensation, it is known that the robot can move along the desired position, so the error compensation and control of the robot is realized, which proves that this method is effective for improving the motion accuracy of the robot. It provides an effective method for improving the motion accuracy of robots. However, the method of controlling the driving angle needs to be explored further.

Author Contributions: D.S. was responsible for the data analysis and manuscript writing. Y.L. (Yu Li) was responsible for the data mining from the literature. Y.L. (Yue Liu) proposed the idea and was responsible for the literature search. S.C. was responsible for the article editing.

Funding: This research was funded by the National Natural Science Foundation of China (Science Foundation) (no. 51834006 and no. 11802035) and the Fundamental Research Funds for the Central Universities (no. 2019QJ002 and no. 2011YJ01).

Conflicts of Interest: The authors declare no conflict of interest.

Appendix A

The displacement data in three directions in three cases.

In x Direction (mm)			In y Direction (mm)			In z Direction (mm)		
Before compensation	After compensation	Ideal displacement	Before compensation	After compensation	Ideal displacement	Before compensation	After compensation	Ideal displacement
-1.5263	0	0	-509.35	-499.8110	-500	-0.2305	0	0
5.3549	6.1959	6.2374	-511.25	-501.8099	-502	0.1247	1.0296	0.6556
11.919	12.0423	12.2021	-513.15	-503.8089	-504	1.7888	3.3249	2.5936
17.9055	17.2838	17.6336	-515.05	-505.8078	-506	4.6895	6.7856	5.7295
23.0769	21.6912	22.2943	-516.95	-507.8067	-508	8.7000	11.2604	9.9261
27.2295	25.0719	25.9808	-518.85	-509.8056	-510	13.6455	16.5537	15.0000
30.2022	27.2782	28.5317	-520.75	-511.8045	-512	19.3101	22.4343	20.7295
31.8836	28.2136	29.8357	-522.65	-513.8034	-514	25.4468	28.6451	26.8641
32.2166	27.8373	29.8357	-524.55	-515.8023	-516	31.7880	34.9147	33.1359
31.2012	26.1657	28.5317	-526.45	-517.8012	-518	38.0571	40.9690	39.2705
28.8945	23.2719	25.9808	-528.35	-519.8001	-520	43.9809	46.5435	45.0000
25.4079	19.2823	22.2943	-530.25	-521.7990	-522	49.3014	51.3944	50.0739
20.9025	14.3713	17.6336	-532.15	-523.7979	-524	53.7870	55.3099	54.2705
15.5820	8.7536	12.2021	-534.05	-525.7968	-526	57.2425	58.1188	57.4064
9.6839	2.6746	6.2374	-535.95	-527.7958	-528	59.5181	59.6983	59.3444
3.4688	-3.6000	0	-537.85	-529.7947	-530	60.5155	59.9794	60.0000
-2.7908	-9.7958	-6.2374	-539.75	-531.7937	-532	60.1923	58.9498	59.3444
-8.8221	-15.6423	-12.2021	-541.65	-533.7927	-534	58.5642	56.6545	57.4064
-14.3646	-20.8837	-17.6336	-543.55	-535.7917	-536	55.7035	53.1938	54.2705
-19.1808	-25.2911	-22.2943	-545.45	-537.7908	-538	51.7370	48.7190	50.0739
-23.0670	-28.6718	-25.9808	-547.35	-539.7898	-540	46.8395	43.4256	45.0000
-25.8621	-30.8781	-28.5317	-549.25	-541.7889	-542	41.2269	37.5450	39.2705
-27.4547	-31.8135	-29.8357	-551.15	-543.7879	-544	35.1462	31.3343	33.1359
-27.7877	-31.4372	-29.8357	-553.05	-545.7870	-546	28.8650	25.0647	26.8641
-26.8611	-29.7656	-28.5317	-554.95	-547.7860	-548	22.6599	19.0104	20.7295
-24.7320	-26.8718	-25.9808	-556.85	-549.7851	-550	16.8041	13.4360	15.0000
-21.5118	-22.8822	-22.2943	-558.75	-551.7841	-552	11.5556	8.5850	9.9261
-17.3616	-17.9712	-17.6336	-560.65	-553.7831	-554	7.1460	4.6695	5.7295
-12.4851	-12.3535	-12.2021	-562.55	-555.7821	-556	3.7705	1.8606	2.5936
-7.1198	-6.2745	-6.2374	-564.45	-557.7812	-558	1.5789	0.2811	0.6556
-1.5263	0	0	-566.35	-559.7801	-560	0.6695	0	0

References

1. Der-Ming, K. Direct displacement analysis of a Stewart platform mechanism. *Mech. Mach. Theory* **1999**, *34*, 453–465. [[CrossRef](#)]
2. Mahmood, M.; Mostafa, T.M.; Rasool, N. Kinematic Analysis and Design of a 3-DOF Translational Parallel Robot. *Int. J. Autom. Comput.* **2017**, *14*, 432–441.
3. Hunt, K.H. Structural Kinematics of In-Parallel-Actuated Robot-Arms. *ASME J. Mech. Transm. Autom. Des.* **1983**, *105*, 705–712. [[CrossRef](#)]

4. Korayem, M.H.; Tourajizadeh, H. Maximum DLCC of Spatial Cable Robot for a Predefined Trajectory within the Workspace Using Closed Loop Optimal Control Approach. *J. Intell. Robot. Syst.* **2011**, *63*, 75–99. [[CrossRef](#)]
5. Dai, Z.; Sheng, X.; Hu, J.; Wang, H.; Zhang, D. *Design and Implementation of Bezier Curve Trajectory Planning in DELTA Parallel Robots*; Springer International Publishing: Berlin, Germany, 2015.
6. Qiu, H.; Li, Y.; Li, Y.B. A new method and device for motion accuracy measurement of NC machine tools. Part 1: Principle and equipment. *Int. J. Mach. Tools Manuf.* **2001**, *41*, 521–534. [[CrossRef](#)]
7. Tsai, L.W.; Walsh, G.C.; Stamper, R.E. Kinematics of novel three DOF translational platforms. In Proceedings of the IEEE International Conference on Robotics and Automation, Minneapolis, MN, USA, 22–28 April 1996; pp. 3446–3451.
8. Xu, D.T. Kinematic reliability and sensitivity analysis of the modified Delta parallel mechanism. *Int. J. Adv. Robot. Syst.* **2018**, *15*, 1–8. [[CrossRef](#)]
9. Bai, P.J.; Mei, J.P.; Huang, T. Kinematic calibration of Delta robot using distance measurements. *Proc. Inst. Mech. Eng. Part C J. Mech. Eng. Sci.* **2016**, *230*, 414–424. [[CrossRef](#)]
10. Zhou, W.; Liao, W.H.; Tian, W. Theory and experiment of industrial robot accuracy compensation method based on spatial interpolation. *J. Mech. Eng.* **2013**, *49*, 42–48. [[CrossRef](#)]
11. Zhou, W.; Liao, W.H.; Tian, W.; Wan, S.M.; Liu, Y. Method of industrial robot accuracy compensation based on particle swarm optimization neural network. *China Mech. Eng.* **2013**, *24*, 174–179.
12. Peng, G.Y. Research on Positioning Accuracy Analysis and Error Compensation of Joint Industrial Robot. Ph.D. Thesis, Xi'an University of Architecture and Technology, Xi'an, China, 2017.
13. Peter, V.; Reymond, C. Kinematic calibration of the parallel Delta robot. *Robotica* **1998**, *16*, 207–218.
14. Wang, D.; Bai, Y.; Zhao, J. Robot manipulator calibration using neural network and a camera-based measurement system. *Trans. Inst. Meas. Control* **2012**, *34*, 105–121. [[CrossRef](#)]
15. Gonzalez, E.J.; Cruz, S.R.; Seelinger, M.J.; Cervantes, J.J. An efficient multi-camera multi-target scheme for the three-dimensional control of robot using uncalibrated vision. *Robot. Comput. Integr. Manuf.* **2003**, *19*, 387–400. [[CrossRef](#)]
16. Qu, W.W.; Dong, H.Y.; Ke, Y.L. Pose accuracy compensation technology in robot-aided aircraft assembly drilling process. *J. Aeronaut.* **2011**, *32*, 1951–1960.
17. Lee, S.J. Determination of probabilistic properties of velocities and accelerations in kinematic chains with uncertainty. *J. Mech. Des.* **1991**, *113*, 84–90. [[CrossRef](#)]
18. Wang, J.S.; Bai, J.W.; Gao, M.; Zheng, H.J.; Li, T.M. Accuracy analysis of joint-clearances in a Stewart platform. *J. Tsinghua Univ. (Nat. Sci. Ed.)* **2002**, *42*, 758–761.

